

Technique for an Accurate Estimation of the Mean Square Electric Field in ATR FT-IR Spectroscopy

SANONG EKGASIT

Process Development Laboratory, Thailand Institute of Scientific and Technological Research, Bangkok 10900, Thailand

Index Headings: ATR FT-IR spectroscopy; Mean square electric field; Evanescent field; Kramers-Kronig analysis; Phase change upon reflection.

INTRODUCTION

Spectral intensities in attenuated total reflection Fourier transform infrared (ATR FT-IR) spectroscopy are strongly dependent on both the experimental parameters (i.e., degree of polarization and angle of incidence) and material characteristics (i.e., refractive index of the ATR crystal and complex refractive index of the material).¹⁻¹⁰ The ATR spectral intensity can be expressed in terms of the product among the mean square electric field (MSEF), refractive index, and extinction coefficient of the absorbing medium. The relationship between the

spectral intensity and the complex refractive index is, generally, nonlinear. This is due to the fact that the MSEF is strongly dependent on the index, and it can be obtained only if the index is known.¹¹⁻¹⁴

Under nonabsorbing conditions (i.e., the extinction coefficient equals zero), the MSEF can be calculated and is given a special name as *the mean square evanescent field* (MSEvF). The expression for the MSEvF under various experimental conditions is given elsewhere.^{4,7,9}

Under a weakly absorbing condition, the MSEF can be estimated from the MSEvF, and a linear relationship between the spectral intensity and the extinction coefficient can be assumed. Under such a condition, a quantitative analysis can be performed since the spectral intensity is directly proportional to the concentration of the material (which is expressed in terms of the extinction coefficient or absorption coefficient).

Under a strongly absorbing condition (i.e., when the

Received 18 July 1997; accepted 22 January 1998.

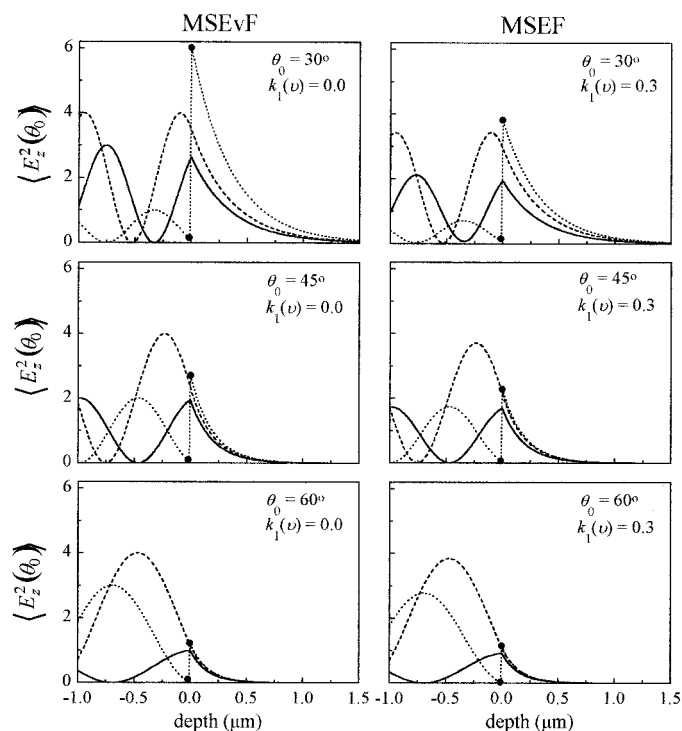


FIG. 1. The MSEvF and the MSEF at various angles of incidence [$\langle E_{zx}^2(\theta_0, \nu) \rangle$ (solid lines), $\langle E_{zy}^2(\theta_0, \nu) \rangle$ (dash lines), and $\langle E_{zz}^2(\theta_0, \nu) \rangle$ (dotted lines)]. The optical parameters are $n_0 = 4.0$, $n_1 = 1.5$, and $\nu = 1700 \text{ cm}^{-1}$. The filled circles indicate the discontinuities of the electric fields in the z coordinate.

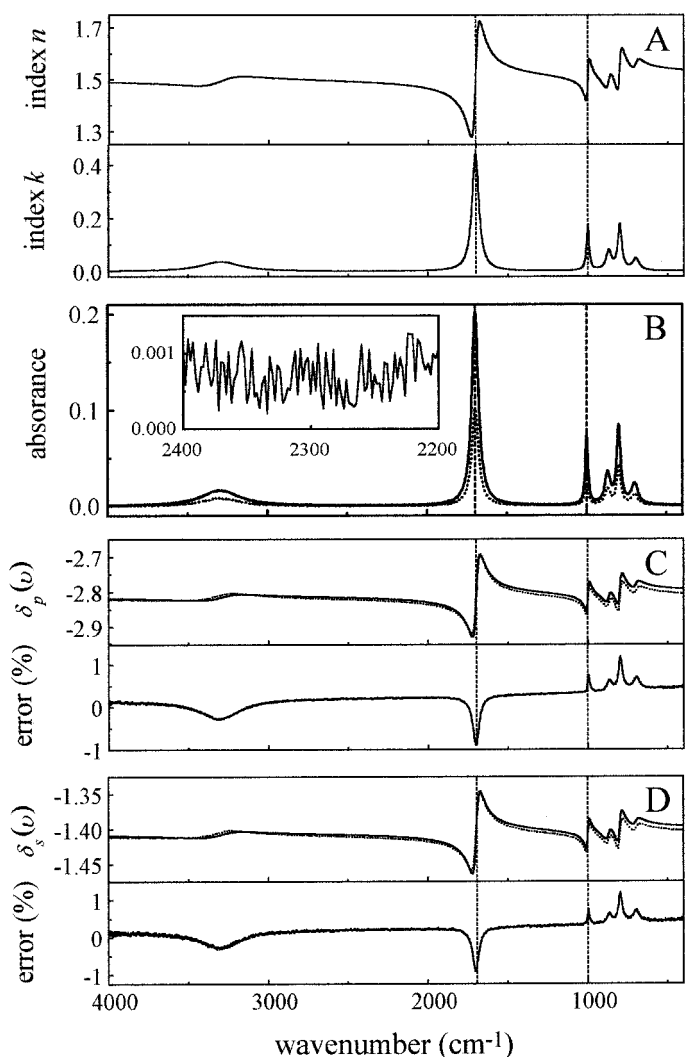


FIG. 2. The complex refractive index spectrum of the model material (A) and noise-added ATR spectra (B) of the material with p -polarization (solid line) and s -polarization (dash line); $n_0 = 4.0$ and $\theta_0 = 45^\circ$. The insert shows the noise level (0.001 a.u.) in a nonabsorbing region of the p -polarized spectrum. Comparisons between phase change upon reflection obtained from exact optical theory (solid line) and those from KK analysis (dash line) of the p -polarized spectrum (C) and the s -polarized spectrum (D).

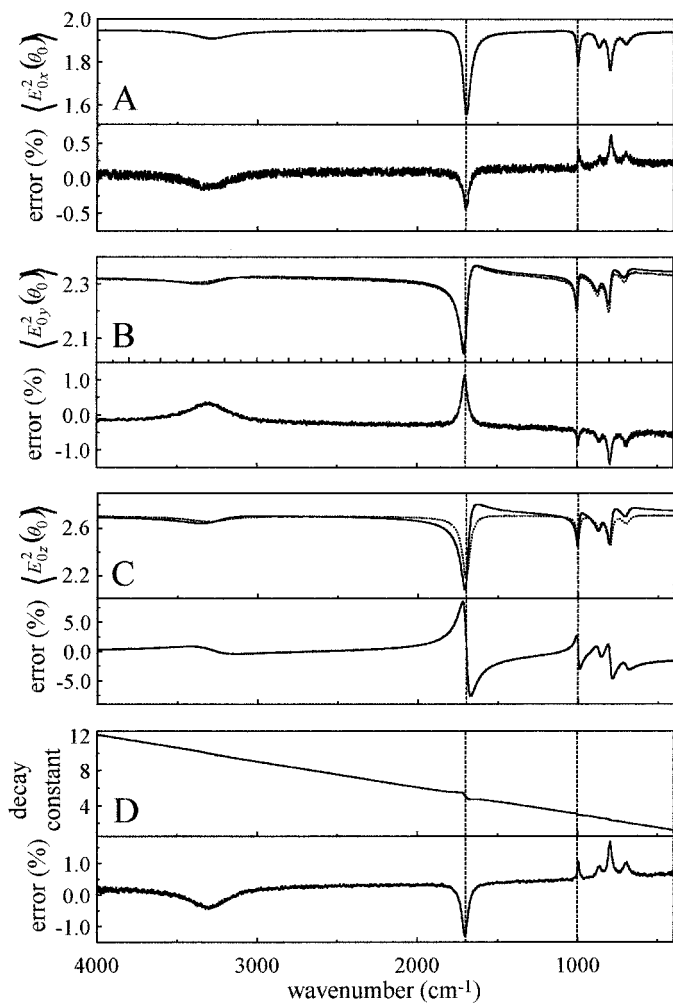


FIG. 3. The MSEFs at the surface in x , y , and z coordinates and their decay constant obtained via exact optical theory (solid lines) and KK analysis (dotted lines); $n_0 = 4.0$ and $\theta_0 = 45^\circ$.

absorption coefficient is large, the angle of incidence is close to the critical angle or the refractive index of the ATR crystal is close to that of the absorbing medium), on the other hand, the MSEF is significantly different from the MSEvF.^{10,12} As a result, the MSEF cannot be accurately estimated from the MSEvF. In order to perform quantitative analysis via a strong absorption band, an accurate value of the MSEF is necessary. Since the complex refractive index of a material is not known, a technique for an accurate estimation of the MSEF from the observed spectral intensity and experimental parameters is required.

DISCUSSION

The theoretical expressions for the MSEFs in terms of the experimental parameters and the physical constants of the material are given in Ref. 11. Examples of the MSEvF and MSEF at various angles of incidences are shown in Fig. 1. The MSEF is always smaller than the MSEvF due to absorption. Although their magnitudes are significantly different, even under weakly absorbing conditions, their decay behaviors are similar.¹² For isotropic media, the decay behaviors of the MSEF in all Cartesian coordinates are characterized by the same function. There

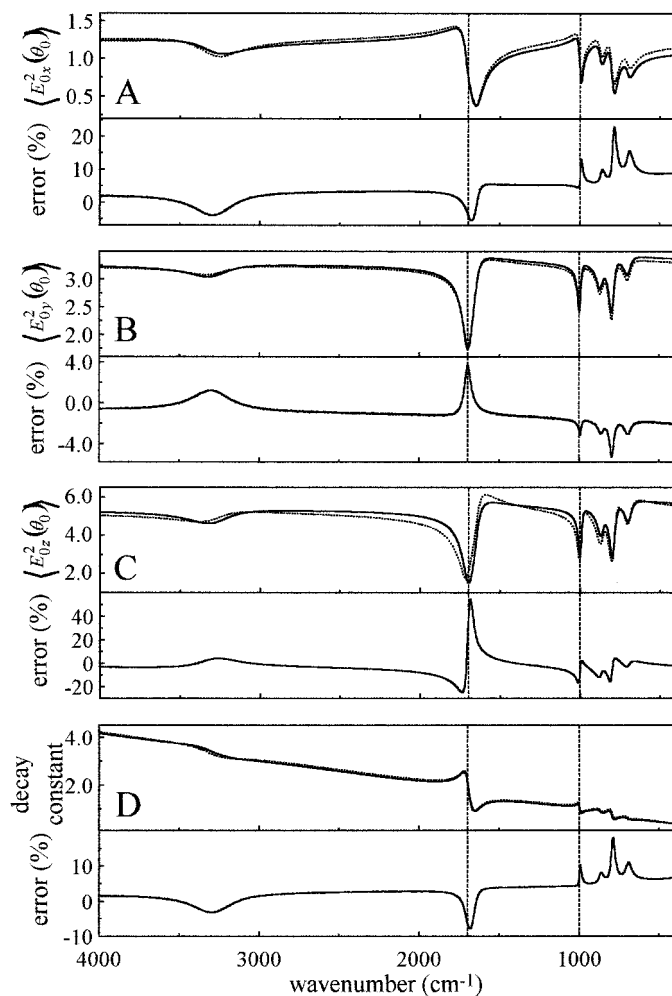


FIG. 4. The MSEFs at the surface and their decay constant. The optical parameters and the symbols are the same as those in Fig. 3 with $n_0 = 2.41$.

are continuities of the MSEFs at the interface in the x and y coordinates, while there is a discontinuity in the z coordinate. By taking advantage of the continuity, one can calculate the fields at the surface of the absorbing media in x and y coordinates from the observed spectral intensity and experimental parameters by the following expressions:¹¹

$$\langle E_{0x}^2(\theta_0, \nu) \rangle = \cos^2\theta_0 [1 + R_p(\theta_0, \nu) - 2R_p^{1/2}(\theta_0, \nu)\cos\delta_p(\nu)] \quad (1)$$

$$\langle E_{0y}^2(\theta_0, \nu) \rangle = 1 + R_s(\theta_0, \nu) + 2R_s^{1/2}(\theta_0, \nu)\cos\delta_s(\nu). \quad (2)$$

Despite the discontinuity, the MSEF at the surface in a z coordinate can be calculated from the observed spectral intensity by

$$\langle E_{0z}^2(\theta_0, \nu) \rangle = \sin^2\theta_0 \frac{n_0^4}{|\hat{n}_1(\nu)|^4} \times [1 + R_p(\theta_0, \nu) + 2R_p^{1/2}(\theta_0, \nu)\cos\delta_p(\nu)] \quad (3)$$

where θ_0 is the angle of incidence, $\langle E_{0j}^2(\theta_0, \nu) \rangle$; $j = x, y, z$ is the MSEF at the surface, $R_l(\theta_0, \nu)$; $l = p, s$ is the reflectance; and $\delta_l(\nu)$ is the phase change upon reflection.

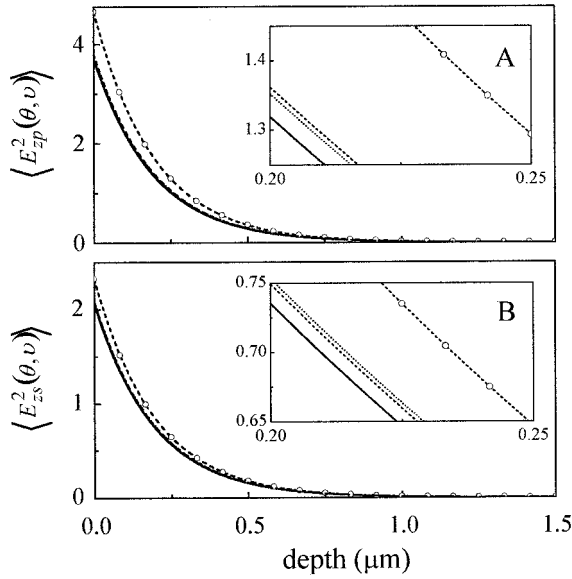


FIG. 5. The MSEvF (dash line with open circle) and the MSEFs obtained via exact optical theory (solid lines), via Eqs. 4 and 5 (dash lines) and via KK analysis (dotted lines) as a function of depth at $\nu = 1700 \text{ cm}^{-1}$, $n_0 = 4.0$, and $\theta_0 = 45^\circ$. The corresponding spectra, phase change upon reflection, and decay constant are shown in Figs. 2 and 3. The inserts are shown for clarity.

Under a weakly absorbing condition, the MSEF can be estimated from the MSEvF since the following assumption can be applied: the decay behavior of the MSEF is the same as that of the MSEvF, and the phase change upon reflection is the same as that under a nonabsorbing condition.^{4,12}

For *s*-polarization:

$$\begin{aligned} \langle E_{0s}^2(\theta_0, \nu) \rangle &\cong 1 + R_s(\theta_0, \nu) + 2R_s^{1/2}(\theta_0, \nu)\cos\delta_{s,k=0} \\ &\cong 1 + R_s(\theta_0, \nu) + 2\left[1 - \frac{1 - R_s(\theta_0, \nu)}{2}\right]\cos\delta_{s,k=0} \\ &\cong (1 + \cos\delta_{s,k=0})[1 + R_s(\theta_0, \nu)] \\ \frac{\langle E_{0s}^2(\theta_0, \nu) \rangle}{\langle E_{0s}^2(\theta_0, \nu) \rangle_{k=0}} &\cong \frac{1 + R_s(\theta_0, \nu)}{2}. \end{aligned} \quad (4)$$

For *p*-polarization:

$$\begin{aligned} \langle E_{0p}^2(\theta_0, \nu) \rangle &\cong \frac{n_0^2}{n_1^2} \left[1 + R_p(\theta_0, \nu) + 2R_p^{1/2}(\theta_0, \nu)\cos\delta_{p,k=0} \right] \\ &\cong \frac{n_0^2}{n_1^2} \left(1 + \cos\delta_{p,k=0} \right) \left[1 + R_p(\theta_0, \nu) \right] \\ \frac{\langle E_{0p}^2(\theta_0, \nu) \rangle}{\langle E_{0p}^2(\theta_0, \nu) \rangle_{k=0}} &\cong \frac{1 + R_p(\theta_0, \nu)}{2}. \end{aligned} \quad (5)$$

It should be noted that $\langle E_{0p}^2(\theta_0, \nu) \rangle = \langle E_{0x}^2(\theta_0, \nu) \rangle + \langle E_{0z}^2(\theta_0, \nu) \rangle$ and $\langle E_{0s}^2(\theta_0, \nu) \rangle = \langle E_{0y}^2(\theta_0, \nu) \rangle$. The phase change upon reflection can be derived from the complex reflection coefficient (which is expressed in terms of the observed spectral intensity) via the following expression:^{11,15–17}

$$\ln \hat{r}_l(\theta_0, \nu) = \ln R_l^{1/2}(\theta_0, \nu) + i\delta_l(\theta_0, \nu). \quad (6)$$

By applying the Hilbert transformation on the above re-

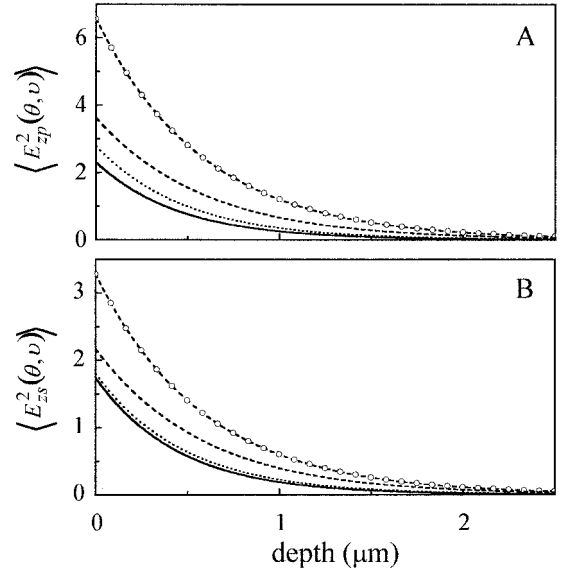


FIG. 6. The MSEvF and the MSEFs obtained from various techniques. The optical parameters and symbols are the same as those in Fig. 5 with $n_0 = 2.41$. The corresponding spectra, phase change upon reflection, and decay constant are not shown.

lationship, we can express $\delta_l(\theta_0, \nu)$ in terms of $R_l(\theta_0, \nu)$ via the Kramers–Kronig (KK) relationship by^{15–17}

$$\delta_l(\theta_0, \nu) = \delta_l^{\text{cor}}(\theta_0) - \frac{2\nu}{\pi} \int_0^\infty \frac{\ln R_l^{1/2}(\theta_0, \nu')}{\nu'^2 - \nu^2} d\nu'. \quad (7)$$

The phase change upon reflection is defined within the region $-\pi \leq \delta_l(\theta_0, \nu) \leq \pi$. $\delta_l^{\text{cor}}(\theta_0)$ is the phase correction term (i.e., phase change at an infinite frequency where the material is not absorbing) and is given under a total internal reflection condition by^{15,16}

$$\delta_p^{\text{cor}}(\theta_0) = 2 \tan^{-1} \left[\frac{n_0 \left(\frac{n_0^2}{n_1^2} \sin^2 \theta_0 - 1 \right)^{1/2}}{n_1 \cos \theta_0} \right] - \pi \quad \text{for } p\text{-polarization} \quad (8A)$$

$$\delta_s^{\text{cor}}(\theta_0) = 2 \tan^{-1} \left[\frac{(n_0^2 \sin^2 \theta_0 - n_1^2)^{1/2}}{n_1 \cos \theta_0} \right] - \pi \quad \text{for } s\text{-polarization.} \quad (8B)$$

Now, the phase change upon reflection can be calculated from the observed spectral intensity. A comparison between the phases obtained via KK analysis and that via an exact equation is shown in Fig. 2. There is a minor difference between the phases due to the added noise and the error in KK analysis.

The MSEF at depth z in an absorbing medium can be characterized by the field at the surface and its decay constant. An accurate decay constant of the MSEF can be calculated from the observed spectrum under *s*-polarization and is given by

$$4\pi\nu \text{Im}[\hat{n}_1(\nu)\cos\hat{\theta}_1] = 4\pi\nu n_0 \cos\theta \text{Im} \left[\frac{1 - \hat{r}_s(\theta, \nu)}{1 + \hat{r}_s(\theta, \nu)} \right]. \quad (9)$$

At a nonabsorbing frequency, the decay constant

can be expressed in terms of the penetration depth by $4\pi\nu \operatorname{Im}[\hat{n}_1(\nu)\cos\theta_1] = 2/d_p(\theta, \nu)$ where $d_p(\theta, \nu) = \{2\pi\nu [n_0^2 \sin^2\theta - n_1^2(\nu)]^{1/2}\}^{-1}$.

By substituting the phase change upon reflection into Eqs. 1–3, we can obtain an accurate value of the MSEF at the surface of an absorbing medium. The MSEFs at the surface in all Cartesian coordinates and their decay constant (corresponding to spectrum in Fig. 2B) are shown in Fig. 3. Examples of the MSEFs for a system with very high absorption are shown in Fig. 4. Large discrepancies between the exact and the estimated fields are observed because of strong absorption.

A comparison among fields in an absorbing medium (Fig. 2A) as a function of depth at 1700 cm^{-1} with Ge and ZnSe as ATR crystals is shown in Figs. 5 and 6, respectively. Under a strong absorption (i.e., Fig. 6), MSEFs obtained via Eqs. 4 and 5 are significantly different from those obtained via the exact equations.¹¹ This result is due to large discrepancies between the strength at the surface and the decay constant of the MSEF and those of the MSEvF. The results obtain via KK analysis,

on the other hand, are more accurate (although there are minor differences between the fields due to the error in phase change upon reflection obtained via KK analysis).

1. N. J. Harrick, *J. Opt. Soc. Am.* **55**, 85 (1965).
2. W. N. Hansen, *Spectrochim. Acta* **21**, 815 (1965).
3. P. A. Flournoy and W. J. Schaffers, *Spectrochim. Acta* **22**, 5 (1966).
4. W. N. Hansen, in *Advances in Electrochemistry and Electrochemical Engineering*, R. H. Muller, Ed. (John Wiley, New York, 1973), Vol. 9.
5. H. G. Tompkins, *Appl. Spectrosc.* **28**, 335 (1974).
6. T. Hirschfeld, *Appl. Spectrosc.* **31**, 289 (1977).
7. N. J. Harrick, *Internal Reflection Spectroscopy* (Harrick Scientific Corporation, Ossining, New York, 1987).
8. L. J. Fina, *Appl. Spectrosc. Rev.* **29**, 309 (1994).
9. F. M. Mirabella, Jr., *Appl. Spectrosc. Rev.* **21**, 45 (1985).
10. S. Ekgasit and H. W. Siesler, *Appl. Spectrosc.* **52**, xxx (1998).
11. W. N. Hansen, *J. Opt. Soc. Am.* **58**, 380 (1968).
12. S. Ekgasit and H. Ishida, *Appl. Spectrosc.* **50**, 1187 (1996).
13. S. Ekgasit and H. Ishida, *Vib. Spectrosc.* **13**, 1 (1997).
14. S. Ekgasit and H. Ishida, *Appl. Spectrosc.* **51**, 461 (1997).
15. K. Yamamoto, A. Masui, and H. Ishida, *Appl. Opt.* **33**, 6285 (1994).
16. K. Yamamoto and H. Ishida, *Spectrochim. Acta* **50A**, 2079 (1966).
17. K. Yamamoto and A. Masui, *Appl. Spectrosc.* **49**, 639 (1995).